ELSEVIER

Wear 250 (2001) 293–298

WEAR

www.elsevier.com/locate/wear

Sliding speed-temperature wear transition maps for Si_3N_4/iron alloy couples

J.R. Gomes [a], A.S. Miranda [a], J.M. Vieira [b], R.F. Silva [b,*]

[a] *Department of Mechanical Engineering, University of Minho, 4800-058 Guimarães, Portugal*
[b] *Department of Ceramics and Glass Engineering, UIMC, University of Aveiro, 3810-193 Aveiro, Portugal*

Abstract

The superior high temperature resistance of silicon nitride (Si_3N_4) based ceramics makes them suitable for tribological applications above room temperature or in high speed unlubricated sliding. There are some published works on the wear behaviour of Si_3N_4/metal alloys. However, experimental data are shown in a form that is not of direct use for engineers involved in materials selection. In the present work, Si_3N_4 pins were tested against tool steel and grey cast iron on a pin-on-disc tribometer. Ceramics were produced by hot-pressing and tested without lubrication at variable temperature and sliding speed. SEM/EDS and XRD analysis were used for chemical and microstructural characterisation of worn surfaces and wear debris. At low speeds (0.05–0.5 m s^{-1}) and room temperature, Si_3N_4 surfaces are polished-like due to a combination of humidity-assisted tribo-oxidation and abrasive action of very fine wear debris. At high sliding speeds (2–3.5 m s^{-1}), as well as for temperatures in the range 400–600°C, an extensive coherent tribolayer mainly composed by iron oxides spreads over the ceramic surfaces. Polishing and protection by adherent tribolayers are the mechanisms responsible for observed severe and mild wear regimes, respectively. Wear maps are constructed showing the transition of wear regimes in Si_3N_4/iron alloys contacts determined by constant flash temperature curves. Equations for calculation of bulk and flash contact temperatures in tribocontacts between dissimilar materials are deduced.

Keywords: Wear maps; Silicon nitride; Flash temperature; Tribolayer

1. Introduction

Graphical presentations of wear phenomena have been thoroughly presented in the literature under slightly different perspectives like wear-mode, wear-mechanism, wear-transition maps, among other designations [1–11]. The interest of these diagrams is to provide to the engineers and designers a ready access to the behaviour of a tribological system under given sliding conditions. Lim, in a recent work [1], referred to the terminology used to distinguish such diagrams, describing their chronological evolution, and pointed out to future directions in wear mapping. About 13 years ago, Lim and Ashby [2] led the way to the comprehensive construction of wear-mechanism maps, showing the wear rate and the regime of wear mechanism dominance in steel/steel tribocontacts over a wide range of load and sliding speeds. Still, the most part of the published wear maps have continued to report on the wear behaviour of metals but the concept was extended to other materials, namely ceramics [3–11]. Some of these works were related to silicon nitride (Si_3N_4) self-mated experiments [5,6,8–10]. However, the presentation of wear maps of Si_3N_4 in dissimilar contacts with metals is very scarce and, to our knowledge, only one paper was published on the subject [12]. In that work, Si_3N_4 ball-on-steel disc wear testing was accomplished at room temperature in the sliding speed and normal load ranges of 0.013–2.3 m s^{-1} and 2.3–100 N, respectively. For the ceramic material, load–velocity experimental wear diagrams were presented denoting three wear regimes: (i) a low speed/low load regime (e.g.: $v < 0.1$ m s^{-1}, $F_n < 10$ N) governed by the tribochemical wear of the ceramic; (ii) an intermediate regime where the ceramic surface appears very polished (attributed to transgranular fracture), showing a wear coefficient in the order of 10^{-5} mm^3 N^{-1} m^{-1}, similarly to the first regime; (iii) a high speed/high load regime (e.g.: $v > 3$ m s^{-1}, $F_n > 30$ N) where a protective layer from transferred steel debris covers the Si_3N_4 ball causing an order-of-magnitude wear decreasing.

The purpose of the present work is to depict in the form of a wear map, the wear mechanisms of Si_3N_4 against two iron alloys, tool steel and grey cast iron. The plotted axis are experimental variables sliding speed and test temperature and the inside contours are the calculated contact flash temperatures. We have called it a wear transition map due to

* Corresponding author. Tel.: +351-2344-370-243; fax: +351-234-425-300.
E-mail address: rsilva@cv.ua.pt (R.F. Silva).

0043-1648/01/$ – see front matter
PII: S0043-1648(01)00594-4

its likeness to the wear transition diagrams of Dong and Jahanmir [6,7], where a large transition zone appears between distinct controlling mechanism regions.

2. Experimental

Silicon nitride (SN) ceramic conical pins (⌀ 1 mm flat ended) were tested against tool steel (TS) and grey cast iron (GCI) discs (⌀ 75 mm) in a pin-on-disc tribometer. Testing parameters were: (i) sliding speed, v, in the range 0.05–3.5 m s^{-1}; (ii) disc temperature, T, from room value up to 600°C. Experiments were performed without lubrication at a constant load, F_n, of 5 N. Testing details, compositions and mechanical properties of the ceramic pins and metallic discs were reported elsewhere [13,14].

The pin wear coefficients, K, were calculated in the steady state wear regime as $K = V/(F_n x)$, V being the wear volume and x the sliding distance. Sliding distances varied between 3 and 42 km. Wear coefficient average and standard deviation values were assessed by measuring the pin weight loss after intermediate stopping of the tests. Friction values, f, were also calculated dividing the tangential friction force, F_f, measured with a bend-type loading cell, by the normal load, $f = F_f/F_n$. The friction coefficient was estimated as the average value of the results taken in those partial runs. The worn surfaces of the pins, the track surfaces of the discs and the wear debris were characterised by using scanning electron microscopy (SEM) with chemical analysis (EDS). The amorphous or the crystalline nature of the wear debris was assessed by X-ray diffraction (XRD) analysis.

3. Results and discussion

3.1. Friction and pin wear coefficients

Experimental values of friction and pin wear coefficients for the SN/TS and SN/GCI sliding pairs are summarised in Table 1. At room temperature, for both metallic contact situations, the pin wear decreases one order of magnitude from the slower velocities, 0.05–0.5 m s^{-1}, to the high sliding speed range, 2–3.5 m s^{-1}. The same tendency is observed from room to the higher temperature testing, the steeper decreasing being observed in the 22–200°C range. Friction coefficients presented in Table 1 were not substantially affected by the testing conditions. Average values for SN/TS and SN/GCI contacts are $f = 0.81 \pm 0.06$ and $f = 0.70 \pm 0.13$, respectively.

3.2. Tribolayer protection of ceramic surfaces

The observation of the morphologies of the ceramic worn surfaces of both the SN/TS and SN/GCI experiments show three different regimes of behaviour related to a tribolayer formation in contact against both iron alloys: (I) at low speeds, 0.05–0.5 m s^{-1} and at room temperature, SN surfaces are polished with a smooth appearance, being free of adherent debris, Fig. 1(a); (II) in the low speed regime and at intermediate temperatures, 100 and 200°C, the ceramic surfaces are partially covered by an incoherent (not aggregated) layer of wear debris, Fig. 1(b); (III) at high sliding speeds, 2–3.5 m s^{-1} as well as for 400–600°C, an extensive coherent tribolayer is spreading along the ceramic surfaces, Fig. 1(c) and (d). Micrographs in Fig. 1 are similarly aligned to keep the sliding direction of the opposite surface from left to right.

Table 1
Pin wear coefficients, K, and friction coefficients, f, for pin-on-disc sliding experiments of silicon nitride (SN) against tool steel (TS) and grey cast iron (GCI) at different sliding speeds, v, and ambient temperatures, T

Pin/disc	v (m s^{-1})	T (°C)	K (10^{-6} mm^3 N^{-1} m^{-1})	f
SN/TS				
	0.05	22	16.3 ± 0.3	0.80 ± 0.07
	0.2	22	14.6 ± 0.6	0.82 ± 0.03
	0.5	22	8.7 ± 0.3	0.72 ± 0.02
		100	6.5 ± 0.3	0.89 ± 0.03
		200	3.9 ± 0.2	0.84 ± 0.01
		400	2.5 ± 0.2	0.78 ± 0.02
		600	2.0 ± 0.6	0.73 ± 0.14
	2	22	2.9 ± 0.1	0.85 ± 0.04
	3.5	22	1.9 ± 0.1	0.82 ± 0.04
		200	4.9 ± 0.3	0.87 ± 0.07
SN/GCI				
	0.05	22	18.3 ± 0.5	0.63 ± 0.04
	0.2	22	16.6 ± 0.4	0.72 ± 0.05
	0.5	22	15.5 ± 0.4	0.74 ± 0.01
		100	5.2 ± 0.1	0.93 ± 0.10
		200	3.2 ± 0.1	0.80 ± 0.02
		400	0.8 ± 0.1	0.48 ± 0.04
		600	1.5 ± 0.2	0.79 ± 0.09
	2	22	5.5 ± 0.2	0.67 ± 0.04
	3.5	22	1.7 ± 0.1	0.51 ± 0.03
		200	1.2 ± 0.1	0.69 ± 0.10

Typical EDS and XRD spectra for the tribolayer and the loose wear debris were already presented in previous works on the room temperature [13] and elevated temperature [14] wear behaviour of SN/iron alloys contacts. In summary, at room temperature with slow sliding speeds, the wear debris are mostly composed by amorphous silica and ferrite with traces of α-Si_3N_4. At elevated temperatures or high sliding speeds, spinel oxide (Fe_3O_4) and the rhombohedral oxide (α-Fe_2O_3) are the main constituents. When a tribolayer is present, its composition has the same oxidised metal nature of the wear debris and it appears as a white film in SEM backscattering imaging, Fig. 1(d).

The wear behaviour of the Si_3N_4 ceramic pins in sliding against the iron alloys was reported to be controlled by the formation and protection afforded by this tribofilm, transferred from the opponent disc oxidised surface in tests above room temperature or above 0.5 m s^{-1} [13,14]. The wear coefficients of the metallic counterparts ranged between

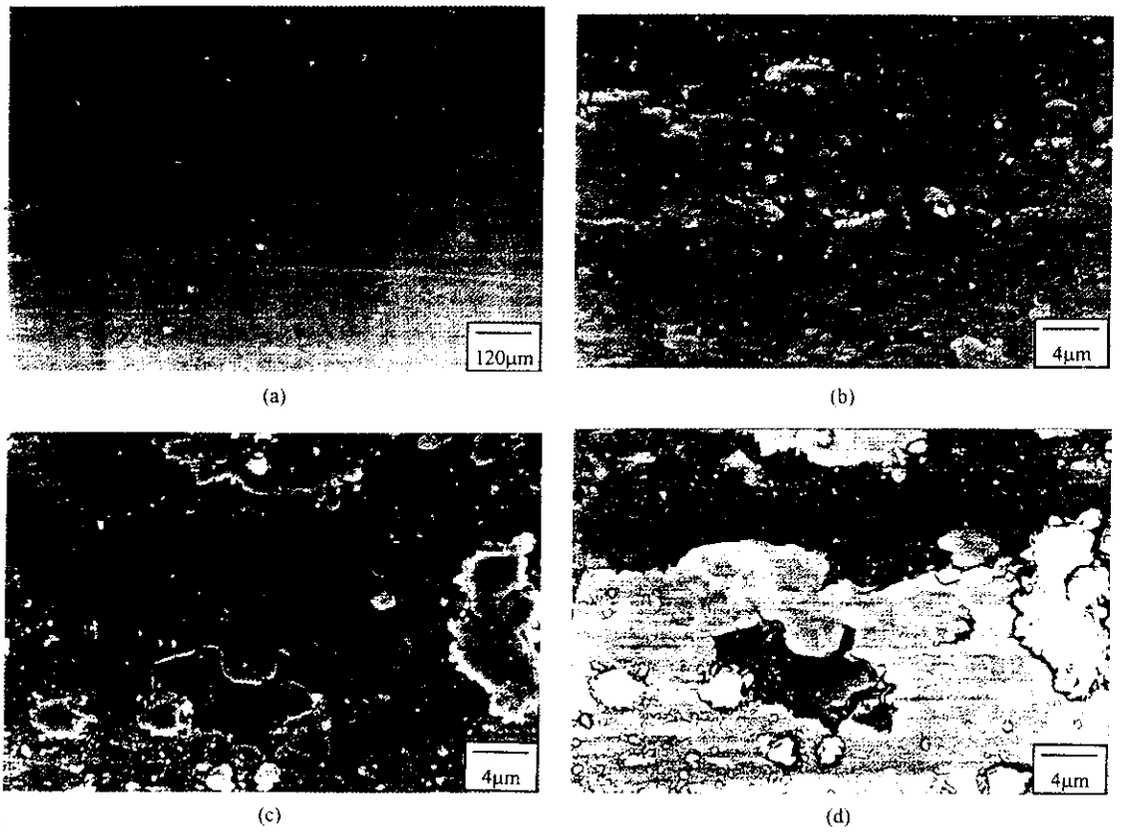

Fig. 1. SEM micrographs of Si_3N_4 pin surfaces after sliding on tool steel discs for the following test conditions: (a) $T = 22°C$ and $v = 0.5\,m\,s^{-1}$ (SE image); (b) $T = 200°C$ and $v = 0.5\,m\,s^{-1}$ (SE image); (c) $T = 22°C$ and $v = 3.5\,m\,s^{-1}$ (SE image); (d) the same as in (c) but BS image.

4.0×10^{-6} and $7.3 \times 10^{-5}\,mm^3\,N^{-1}\,m^{-1}$ [13,14]. The effectiveness of this layer increases with the local contact temperature that is directly related to the sliding speed or the test temperature. Protection afforded by this adherent tribolayer, known as third body protection [15], is efficient in regime (III), where thick continuous and relative homogeneous adherent layers diminish the local loads on the ceramic surfaces by redistributing the contact stresses, reducing mechanical damaging. Simultaneously, severe disc wear occurs, the sacrificial action of this metallic counterface leading to decreasing values of the ceramic pin wear coefficient [13,14].

In the absence of the tribolayer protection, regime (I), the ceramic surface appears polished as a result of the combination of humidity-assisted tribo-oxidation and very fine abrasion modes [13]. In this regime, the ceramic wear coefficient is higher against the GCI material comparing to sliding on the TS discs. This was attributed to the effect of disc topography: graphite pull out on the GCI disc lead to a rougher surface than for the TS material and to increasing contact severity [13]. In contrast, in the presence of a tribolayer, regimes (II) and (III), the ceramic wear resistance against GCI tends to level with K results against TS, Table 1 (see results above 22°C and/or above $0.5\,m\,s^{-1}$) due to the similar nature and effect of the tribolayer.

3.3. Wear mode dependence on flash temperatures

The results from the pin-on-disc tests show that sliding speed and test temperature are experimental parameters that determine the tribological behaviour of the tested materials. In previous works [13,14], the effect of each parameter was deeply but separately discussed. The purpose of the present work is to look for such dependence in a combined way by calculating the two well known figures of contact temperature between the mating surfaces, the so-called bulk temperature, T_b, and the flash temperature, T_f [2]. The latter can attain very high values, in the order of several thousands of celsius degrees [2,9,16], making it a crucial parameter to the morphological evolution of the sliding surfaces.

Well-established definitions of these temperatures are given in the work of Lim and Ashby [2] for homologous surfaces. However, the present work relates to the tribological contact between ceramic and metallic surfaces. The equations of the reported pioneer work of Lim and Ashby cannot be directly used and the heat partition between dissimilar pin and disc materials has thus to be solved, considering the different physical properties, namely thermal, for both materials. The following new definition for T_b, Eq. (1), was step-by-step deduced similarly to the referred paper. The equation for T_f, Eq. (2), results equal to the one

Table 2
Symbols, definitions and values of variables used for bulk and flash temperature calculations

Symbol	Definition (units)	Value
T_b	Bulk temperature (K)	(Final result for each test condition)
T_0	Sink temperature (K)	Test temperature
f	Friction coefficient	0.81 and 0.70, respectively for SN/TS and SN/GCI contacts
β	Dimensionless parameter	1 [2]
T_p^*	Pin equivalent temperature (K)	(Value for each test condition)
$\tilde{F}_p$	Pin normalised force (dimensionless)	3.6×10^{-4}
$\tilde{v}_p$	Pin normalised velocity (dimensionless)	(Value for each test condition)
$K_{m,p}$	Thermal conductivity of the pin ($W\,m^{-1}\,K^{-1}$)	30 [17]
$K_{m,d}$	Thermal conductivity of the disc ($W\,m^{-1}\,K^{-1}$)	27 for TS [18] and 45 for GCI [19]
$\tilde{v}_d$	Disc normalised velocity (dimensionless)	(Value for each test condition)
T_f	Flash temperature (K)	(Final result for each test condition)
N	Total number of contacting asperities	(Value for each test condition)
a_p	Pin thermal diffusivity ($m^2\,s^{-1}$) for calculation of T_p^* and $\tilde{v}_p$	1.85×10^{-5} [17]
H_p	Pin hardness (GPa) for calculation of $\tilde{F}_p$	17.9
A_n	Nominal area of contact (m^2) for calculation of $\tilde{F}_p$	7.85×10^{-7}
a_p	Disc thermal diffusivity ($m^2\,s^{-1}$) for calculation of $\tilde{v}_d$	9.0×10^{-6} for TS [18] and 1.4×10^{-5} for GCI [20]

for self-mated materials [2]. The variables used in these equations are defined in Table 2.

$$T_b = T_0 + \frac{f\beta T_p^*}{(1+K_{m,d}/K_{m,p})+K_{m,d}/K_{m,p}\beta(\pi\tilde{v}_d/8)^{1/2}}\tilde{F}_p\tilde{v}_p \quad (1)$$

$$T_f = T_b + \frac{f\beta T_p^*}{2N^{1/2}}\tilde{F}_p{}^{1/2}\tilde{v}_p \quad (2)$$

The correction on the thermal conductivity due to the formation of an oxide film in the disc, as suggested by Lim and Ashby [2], is not used in the proposed equations because it does not affect the final result. This was attested using a realistic value of approximately 1 μm in thickness for such film, after microstructural observations in SEM, which is in accordance with the oxidation rate value for iron of 0.6 mm per year at 700°C given by West [21]. Also, the dependence of the pin hardness on temperature, which probably is the most affected physical property in metals [2], was taken into account, but the hardness decreasing between 22 and 600°C is irrelevant in the case of these Si_3N_4 based materials [22].

Calculated flash temperatures for the sliding tests of the present work are plotted in Fig. 2 together with the wear coefficients. The direct measurement of T_f is troublesome due to the ephemeral nature of the tribocontacts at the asperity scale and the difficult assessment to the real contact area. There are no measured or calculated values in the literature for Si_3N_4/metal sliding pairs for comparison. Griffioen at al. [16] measured the T_f in Si_3N_4/sapphire contacts by infrared pirometry through a transparent saphire disc. T_f values between 148 and 2703°C are reported, respectively for (4.45 N; 0.305 m s^{-1}) and (8.90 N; 1.53 m s^{-1}), which are in the range of the predicted values in Fig. 2. Skopp et al. [9] calculated the flash temperatures in unlubricated Si_3N_4/Si_3N_4 contacts for room temperature experiments and gave values between 36 and 3261°C for the sliding speed

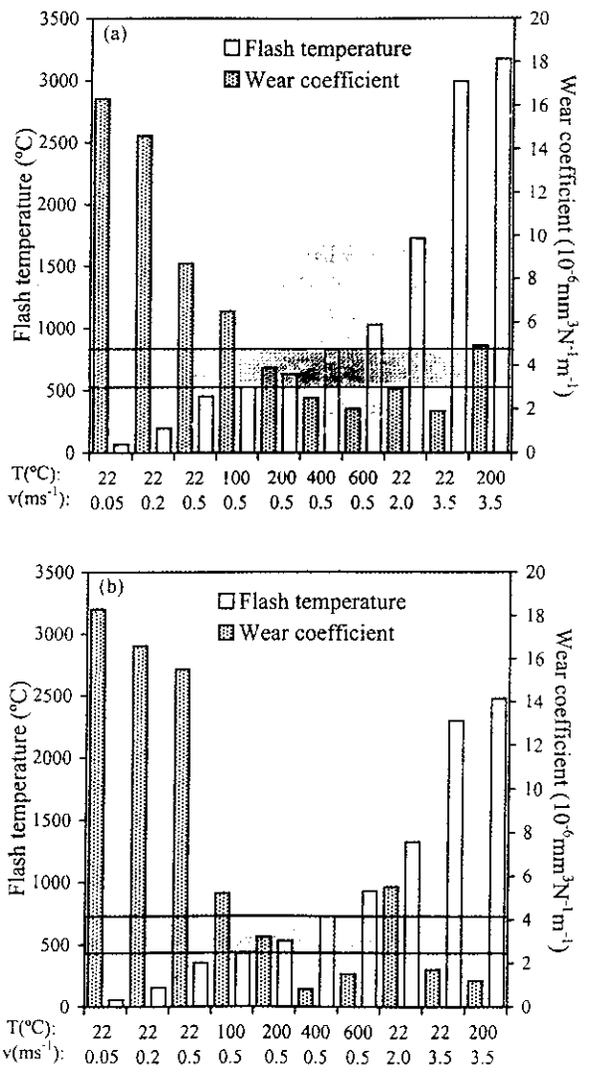

Fig. 2. Wear coefficients and calculated flash temperatures for the complete set of experiments: (a) Si_3N_4/tool steel test; (b) Si_3N_4/grey cast iron tests.

range 0.03–3.0 m s^{-1}, which are quite similar to the present range of 55–3172°C for 0.05–3.5 m s^{-1}.

Ceramic wear coefficients in Fig. 2 varied almost in a reciprocal dependence on the flash temperatures. This is a consequence of the sacrificial action of the metal surface as above reported and supported by other authors [8,23,24]. Well defined wear regimes (I) and (III) and the transition regime (II) described in Section 3.2, can be linked to flash temperature boundaries. Hence, the high wear regime (I), with K values higher than 10^{-5} mm^3 N^{-1} m^{-1}, is observed for test conditions with T_f lower than the value estimated for $T = 100°C/v = 0.5$ m s^{-1}. Such wear coefficients fall in the impractical range for engineering applications [25]. For SN/TS contacts this down-boundary is $T_f = 530°C$ and for SN/GCI contacts it is situated at $T_f = 430°C$. For the low wear regime (III), where third body protection of the ceramic surface is effective and K values approach 10^{-6} mm^3 N^{-1}m^{-1}, up-boundary values of $T_f = 830°C$ for SN/TS pairs and $T_f = 730°C$ for SN/GCI contacts are estimated. Above this, the flash temperature is enough to assure a huge oxidation of the metallic surface, an effective transfer and good adhesion of the oxidised debris to the ceramic surface. The transition regime (II), with intermediate values of T_f, is depicted by the grey shaded regions in Fig. 2(a) and (b). For each given condition, it can be observed that the T_f values for the SN/GCI contacts are slightly lower than for the SN/TS pairs mainly due to the higher thermal conductivity of the grey cast iron material.

3.4. *v–T wear transition maps for Si_3N_4/tool steel and Si_3N_4/grey cast iron*

The T_f boundaries that demarcate the wear regimes (I) and (III) and the transition regime (II) can be plotted in the v–T plane. These wear transition maps, in Fig. 3(a) and (b), respectively for SN/TS and SN/GCI contacts, present the controlling region of each regime and the shaded transition zone. Contours of constant calculated flash temperature are also superimposed. The use of experimental variables v and T is a deliberate user-friendly option that allow the direct prevision of the Si_3N_4 wear behaviour against iron alloys for a set of sliding speed/test temperature conditions. The two diagrams differ in the magnitude of the flash temperature transitions, which are higher for steel due to the reasons above discussed. Comparing the present work with the cited (in the introduction of this paper) single work of Gautier and Kato on the Si_3N_4/steel mapping [12], it can be observed that the polishing and third body protection regimes are coincident. Yet, in the mentioned work, the polishing regime is divided into tribochemical and mechanical dominated regions but in the present work, humidity-assisted tribo-oxidation and fine abrasion modes are not distinguished. However, the wear mechanisms positioning in both maps almost superimpose, if one replace the normal load/sliding speed axes, in the literature reference, by the combination ambient temperature/sliding speed, in the case of the present work.

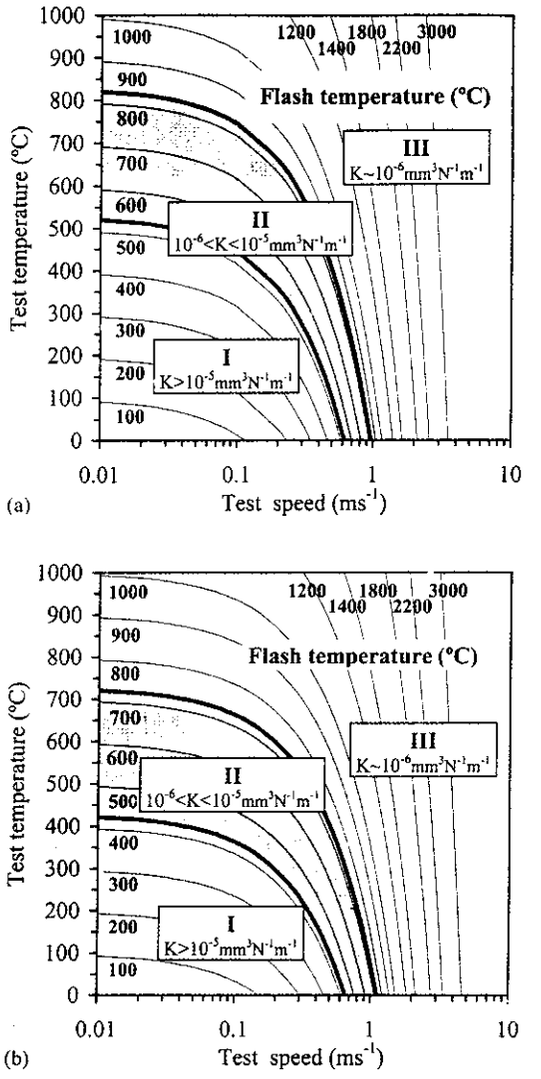

Fig. 3. Wear transition maps for: (a) Si_3N_4/tool steel contacts; (b) Si_3N_4/grey cast iron contacts.

4. Conclusions

The wear behaviour of silicon nitride ceramics in contact with two different iron alloys, tool steel and grey cast iron, is very dependent on experimental parameters, namely sliding speed and ambient temperature. Three distinct wear regimes are observed: (I) a severe wear regime ($K > 10^{-5}$ mm^3 N^{-1} m^{-1}) at room temperature/low speed (0.05–0.5 m s^{-1}), where the ceramic is worn by a combination of humidity-assisted tribo-oxidation and micro-abrasion mechanisms, leading to a polished-like surface; (II) a transition regime, at medium temperatures 100–200°C and low speed, where the ceramic is partially protected by an incoherent layer of transferred oxidised debris from the metal; (III) a mild wear regime ($K \sim 10^{-6}$ mm^3 N^{-1} m^{-1}) at high temperature (400–600°C)/high sliding speed (2–3.5 m s^{-1}) conditions,

where third body protection from an extensive tribolayer is operating.

These wear regimes can be positioned between contact flash temperature (T_f) limits: regime (I) controls the ceramic wear below $T_f = 530$ and $T_f = 430$°C for tool steel and grey cast iron contacts, respectively; above $T_f = 830$ and $T_f = 730$°C for tool steel and grey cast iron contacts, respectively, regime (III) is operating. The wear regimes (I) and (III) and the transition regime (II) are graphically presented in the sliding speed/test temperature plane in the form of wear transition maps with contours of constant calculated flash temperatures.

References

[1] S.C. Lim, Recent developments in wear-mechanism maps, Tribology Int. 31 (1-3) (1998) 87–97.

[2] S.C. Lim, M.F. Ashby, Overview n.55, wear mechanism maps, Acta Metall. 35 (1) (1987) 1–24.

[3] S.M. Hsu, Y.S. Wang, R.G. Munro, Quantitative wear maps as a visualisation of wear mechanism transitions in ceramic materials, Wear 134 (1989) 1–11.

[4] K. Kato, Tribology of ceramics, Wear 136 (1990) 117–133.

[5] K. Hokkirigawa, Wear mode map of ceramics, Wear 151 (1991) 219–228.

[6] X. Dong, S. Jahanmir, Wear transition diagram for silicon nitride, Wear 165 (1993) 169–180.

[7] X. Dong, S. Jahanmir, Wear transition diagram for silicon carbide, Tribology Int. 28 (8) (1995) 559–572.

[8] S.W. Lee, M.C. Shen, S.M. Hsu, Ceramic wear maps: silicon nitride, Key Eng. Mater. 89-91 (1994) 751–756.

[9] A. Skopp, M. Woydt, K.H. Habig, Tribological behaviour of silicon nitride materials under unlubricated sliding between 22 and 1000°C, Wear 181-183 (1995) 571–580.

[10] S.M. Hsu, M.C. Shen, Ceramic wear maps, Wear 200 (1996) 154–175.

[11] K. Adachi, K. Kato, N. Chen, Wear map of ceramics, Wear 203-204 (1997) 291–301.

[12] P. Gautier, K. Kato, Wear mechanisms of silicon nitride, partially stabilised zirconia and alumina in unlubricated sliding against steel, Wear 162-164 (1993) 305–313.

[13] J.R. Gomes, A.S. Miranda, R.F. Silva, J.M. Vieira, Tribological properties of AlN–CeO_2–Si_3N_4 cutting materials in unlubricated sliding against tool steel and cast iron, Mat. Sci. Eng. A 209 (1996) 277–286.

[14] J.R. Gomes, A.S. Miranda, R.F. Silva, J.M. Vieira, Tribo-oxidational effects on friction and wear behaviour of silicon nitride/tool steel and silicon nitride/gray cast iron contacts, J. Am. Ceram. Soc. 82 (4) (1999) 953–960.

[15] M. Godet, Y. Berthier, J. Lancaster, Wear modelling: using fundamental understanding or practical experience? Wear 149 (1991) 325–340.

[16] J.A. Griffioen, S. Bair, W.O. Winer, Infrared surface temperature measurements in a sliding ceramic–ceramic contact, in: Proceedings of the Leeds-Lyon Symposium on Tribology, Butterworth Publishing, Guilford, UK, 1985, pp. 238-245.

[17] G. Ziegler, J. Heinrich, G. Wotting, Relationship between processing, microstructure and properties of dense and reaction bonded silicon nitride, J. Mater. Sci. 22 (1987) 3041–3086.

[18] ASM Handbook, Vol. 18, Friction, Lubrication and Wear Technology, ASM International, 1992, p. 42.

[19] J. Helsing, G. Grimvall, Thermal conductivity of cast iron: models and analysis of experiments, J. Appl. Phys. 70 (3) (1991) 1198–1206.

[20] E. Karawacki, B.M. Suleiman, Dynamic plane source technique for simultaneous determination of specific heat, thermal conductivity and thermal diffusivity of metallic samples, Meas. Sci. Technol. 2 (1991) 744–750.

[21] J.M. West, Basic corrosion and oxidation, 2nd edition, Ellis Horwood Limited, West Sussex, UK, 1992, p. 200.

[22] R.F. Silva, J.M. Vieira, Hot hardness of Si_3N_4-based cutting tools, J. Mater. Sci. 30 (1995) 5531–5536.

[23] M.F. Wani, J. Mukerji, B. Prakash, S. Bandopadhyay, Friction and wear behaviour of hot-pressed SiAlON-steel ball tribopair under reciprocating sliding conditions, Am. Ceram. Soc. Bull. 72 (9) (1993) 82–87.

[24] C. Yin-Qian, D. Xiang-Dong, W. Fu-Xing, C. Qi-Gong, Z. Zhang-Xiao, On the wear mechanisms of sialon and metal in dry sliding, Wear 137 (1990) 175–186.

[25] H.E. Sliney, C. Dellacorte, The friction and wear of ceramic/ceramic and ceramic/metal combinations in sliding contact, Lubric. Eng. 50 (7) (1994) 571–576.